ResearchGate

See discussions, stats, and author profiles for this publication at: https://www.researchgate.net/publication/268035440

Microstructural modifications and properties of SiC nanoparticles-reinforced Sn–3.0Ag–0.5Cu solder...

Article *in* Materials and Design · January 2014

DOI: 10.1016/j.matdes.2014.08.058

CITATIONS
14

READS
140

5 authors, including:

A. A. El-Daly
Zagazig University

45 PUBLICATIONS **785** CITATIONS

SEE PROFILE

Waled Desoky
Zagazig University

11 PUBLICATIONS **49** CITATIONS

SEE PROFILE

M. G. El-Shaarawy
Benha University

36 PUBLICATIONS **279** CITATIONS

SEE PROFILE

A. M. Abdraboh
Benha University

3 PUBLICATIONS **59** CITATIONS

SEE PROFILE

All content following this page was uploaded by Waled Desoky on 09 November 2014.

The user has requested enhancement of the downloaded file. All in-text references underlined in blue are added to the original document and are linked to publications on ResearchGate, letting you access and read them immediately.

Materials and Design xxx (2014) xxx–xxx

Contents lists available at ScienceDirect

Materials and Design

journal homepage: www.elsevier.com/locate/matdes

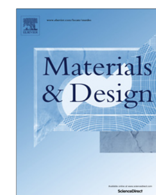

Microstructural modifications and properties of SiC nanoparticles-reinforced Sn–3.0Ag–0.5Cu solder alloy

A.A. El-Daly [a,*], W.M. Desoky [a], T.A. Elmosalami [a], M.G. El-Shaarawy [b], A.M. Abdraboh [b]

[a] Physics Department, Faculty of Science, Zagazig University, Zagazig, Egypt
[b] Physics Department, Faculty of Science, Banha University, Banha, Egypt

ARTICLE INFO

Article history:
Received 16 July 2014
Accepted 25 August 2014
Available online xxxx

Keywords:
Lead-free solders
Microstructure
Mechanical properties

ABSTRACT

Nano-sized SiC particles-reinforced Sn–3.0Ag–0.5Cu (SAC305) composite solder was prepared by mechanically dispersing SiC particles into plain SAC305 alloy at 900 °C for 90 min. The effects of SiC addition on microstructure, melting behavior and tensile properties of as-cast SAC305 solders were systematically investigated. The data from microstructure-properties analysis of composite solder show that the nano-sized SiC particles has significantly refined the microstructure, increased the strength and elastic modulus in comparison with the plain SAC305 solder. In addition, SiC particles decrease the pasty range of composite SAC305-0.7SiC solder although the undercooling and eutectic temperature prolonged nearly at the SAC305 level. A strain rate-dependent model of elastic modulus (E), yield stress (0.2%YS) and ultimate tensile strength (UTS) was developed based on the test results. The predicted tensile parameters for both solders are reasonably close to the present experimental data.

© 2014 Elsevier Ltd. All rights reserved.

1. Introduction

The development of lead-free highly reliable solders has become an important issue for miniaturized electronic interconnection materials due to the toxic nature of Pb–Sn alloys [1]. This advances the electronic packages toward the high density and miniaturization improvement. To address such demanding, ultra-high density packaging technology, nanotechnology and nanoscience should play an important part. Accordingly, one of the new methods for microstructural refinement and enhanced mechanical properties of solder alloys is the modification with nano-sized particles [2]. The particles which are used as modifiers are usually oxides, carbides, or borides with high melting temperature (2000–3000 °C) and average size from 4 to 100 nm. The reinforcing particles should have a small size to suppress the grain growth and therefore assist the formation of small intermetallic compound (IMC). Owing to the microstructure alternation as grain refinement and change in the precipitation morphology, the solder joint could provide better reliability with improved thermal stability of microstructure and mechanical properties [3]. The addition of nano-reinforcements to solder alloys could result in self-organized dispersive systems, which contribute to the heterogeneous nucleation, and strongly increased the part of surface energy of composite solders. Based on these concerns, flurries of activities in electronic community have dedicated to understand the typical reliability issues of Pb-free solder joints. Recently, new improved solders were fabricated by incorporating nanosized, nonreacting, noncoarsening SiC dispersoids into conventional SAC105 solder by El-Daly et al. [4–6]. They reported that the addition of small amount of SiC nanoparticles to SAC105 solder resulted in a finely dispersed submicron Ag_3Sn phase. This apparently provides classical dispersion strengthening and thereby enhances the mechanical strength and reduces the amount of undercooling. Shen et al. [7] elucidated the improvement of mechanical properties and refinement of Ag_3Sn particles in composite Sn–3.5Ag/ZrO_2 solders using the classic theory of dispersion strengthening and the adsorption effect of ZrO_2 nanoparticles, respectively. They also found that ZrO_2 can reduce the undercooling and refines the microstructure of composite solders. Tsao et al. [8,9] developed a series of Sn–3.5Ag–0.25Cu and Sn–3.5Ag–0.5Cu composite solders reinforced with different amounts of TiO_2 and Al_2O_3 nanoparticles. Their results indicated significant enhancement in yield strength, microhardness and ultimate tensile strength with nanoparticles addition. Chuang et al. [10] and Fawzy et al. [11] developed novel composite solders by incorporating Al_2O_3 and ZnO nanoparticles into conventional Sn–3.5Ag–0.5Cu (SAC355) solders. The composite solders were found to have much greater mechanical strength than the plain SAC355 solder. However, no work has been

* Corresponding author. Univ. tel.: +20 552362536, Faculty tel.: +20 552303252, mobile: +20 1271020082; fax: +20 552308213.
E-mail addresses: dreldaly11@yahoo.com, dreldaly@zu.edu.eg (A.A. El-Daly).

http://dx.doi.org/10.1016/j.matdes.2014.08.058
0261-3069/© 2014 Elsevier Ltd. All rights reserved.

ARTICLE IN PRESS

performed on the thermal and mechanical properties of SAC305 composite solder mixed with SiC nanoparticles. The present work examines the microstructure, thermal and mechanical behavior changes that have occurred due to reinforcing SiC nanoparticles while solidifying the SAC305 alloy. The effect of SiC is expected to be sizeable because SiC has no solubility in the β-Sn matrix.

2. Experimental procedures

2.1. Preparation of samples

SAC305 and SAC(305)-0.7% SiC solder alloys were fabricated in nominal weight percent compositions. The chemical compositions of both alloys are listed in Table 1. The crystal size of milled SiC powders (70 nm) was quantified by XRD peak broadening using William–Hall method [5]. Pure tin, silver and copper (99.99 wt.%) were melted in a vacuum furnace at 900 °C for 90 min to produce the plain SAC305 solder alloy. The lead-free composite solder was prepared by mechanically dispersing 0.7 wt.% of SiC nanoparticles into SAC305 solder. In order to get a homogeneous composition within the ingots, the mixture was subsequent re-melted three times in a vacuum furnace at 600 °C for 90 min and then poured in a steel mold to prepare the chill cast ingot. The chill cast with an air-cooling condition of 8.5 °C/s was achieved, so as to create the fine microstructure typically found in small solders joints in microelectronic packages.

2.2. Characterization and metallographic observation of solder samples

The microstructures of both lead-free solder alloys were revealed using scanning electron microscopy (SEM). The specimens were cross-sectioned, ground with sandpaper, polished with 1.0–0.05 μm Al_2O_3 powders, etched with 2%HCl, 3%HNO_3 and 95 vol.% Ethyl alcohol solution. Energy Dispersive X-ray Spectrometry (EDS) was adopted to identify the phase structure of prepared sample alloys. Differential scanning calorimetry (Shimadzu DSC-50) was carried out to identify the melting process of both solder alloys. Heating and cooling the specimens in DSC analysis were carried out at 10 °C/min of heating rate in Ar flow. The solder ingots were then mechanically machined into a wire samples with a gauge length marked 4×10^{-2} m for each samples and 2.5×10^{-3} m in diameter, as developed in our previous work [6]. Before testing, the specimen was annealed at 120 °C for 30 min to reduce the residual stress induced during sample preparation.

2.3. Mechanical testing

Tensile tests were conducted on a 3360 universal material testing system and GWT 504 high temperature testing system, respectively. The tests were carried out at various strain rates ranging from 10^{-4} to 10^{-2} s^{-1} and constant temperature of 25 °C. Also, the tests were conducted at different temperatures ranging from 25 to 120 °C with a constant strain rate. Tensile property data was measured in accordance with the ASTM: D638-10 standard test method for tensile properties of metals. Then, the mechanical properties were obtained by the average of three testing data. The temperature variation inside the high temperature furnace was maintained within 1.5 °C.

3. Results and discussion

3.1. Characterization of SiC nanoparticles

Fig. 1a shows the bright field TEM micrograph of SiC nanoparticles. XRD analysis was performed to determine the phase composition of SiC nanoparticles (Fig. 1b). The TEM micrograph and the observed peak broadening in XRD confirm the presence of nanometric SiC particles. In order to detect the uniform distribution of SiC nanoparticles inside the solder matrix, an over etched SAC(305)-0.7% SiC solder sample was then examined by SEM micrograph, as shown in Fig. 1c. It is interesting to note that the bright spheroids of SiC nanoparticles are distributed uniformly on the surface of dark β-Sn matrix. Thus, the SiC nanoparticles were successfully blended with the SAC305 solder.

3.2. Microstructural characterization of SAC305 and SAC(305)-0.7% SiC solders

The SEM micrographs of SAC305 and SAC(305)-0.7% SiC solder alloys are shown in Fig. 2. The compositions of different phases are shown in the inset of EDS analysis. According to SEM observations in Fig. 2a, the β-Sn dendrites appear to extend directly across the full SEM micrograph of SAC305 solder. The typical coarse needle-like Ag_3Sn phase and irregular polygon of Cu_6Sn_5 phase are exhibits some faceting and large spacing, as revealed in Fig. 2a, consistent with previous results [4–6]. EDS results in Fig. 2c illustrate that the whole surface of solder matrix contains 92.88 at.% Sn, 3.48 at.% Ag and 3.64 at.% Cu elements, which assigned the presence of primary β-Sn, Ag_3Sn and Cu_6Sn_5 IMC phases. Fundamentally, the matrix-strengthening strategy is to avoid or refine β-Sn dendrites, to refine any IMC phases, and to increase the fraction of fine eutectic in the as-solidified solder. Therefore, SiC is being developed to further suppress coarsening of β-Sn matrix and eutectic regions. Fig. 2b clearly shows that the addition of small amount of SiC to SAC305 solder could modify the microstructure of SAC305 solder matrix. The SEM result reveals the grain refining as the most prominent effect of SiC nanoparticles. The rather coarse needle-like Ag_3Sn particles (60–100 μm) with large spacing in Fig. 2a, can be compared to the extremely fine Ag_3Sn (20–60 μm) with small spacing in Fig. 2b. Also, the fine dot Ag_3Sn particles associated with composite solder of Fig. 2b has a very small spacing in the eutectic region. This suggests that the SiC nanoparticles have the ability to serve as either nucleation sites or obstacles to grain growth during solid state cooling. Fig. 2b also shows that the pseudo-eutectic SAC305 solder (shown on the surface of β-Sn phase) contains a large amount of fine dot IMC particles. In addition, the amount of needle-like Ag_3Sn particles increases and spacing between them decreases significantly in the eutectic regions. According to EDS analysis results shown in Fig. 2d, the whole surface area was found to contain 75.32 at.% Sn, 3.48 at.% Ag, 3.64 at.% Cu, 15.14 at.% C and 2.42 at.% Si. Since the composite solder used was SAC(305)-0.7% SiC solder containing SiC nanoparticles, and the Ag_3Sn and Cu_6Sn_5 were the only precipitate phases, it can be concluded that these network eutectic area comprise the fine dot and needle-like Ag_3Sn

Table 1
Chemical composition of the solders studied (wt.%).

Alloy	Cu	Ag	Fe	As	SiC	Sb	In	Sn
SAC(305)	0.501	3.003	0.001	0.001	0.000	0.005	0.002	Bal.
SAC(305)-0.7SiC	0.502	3.004	0.001	0.001	0.704	0.005	0.002	Bal.

Please cite this article in press as: El-Daly AA et al. Microstructural modifications and properties of SiC nanoparticles-reinforced Sn–3.0Ag–0.5Cu solder alloy. J Mater Design (2014), http://dx.doi.org/10.1016/j.matdes.2014.08.058

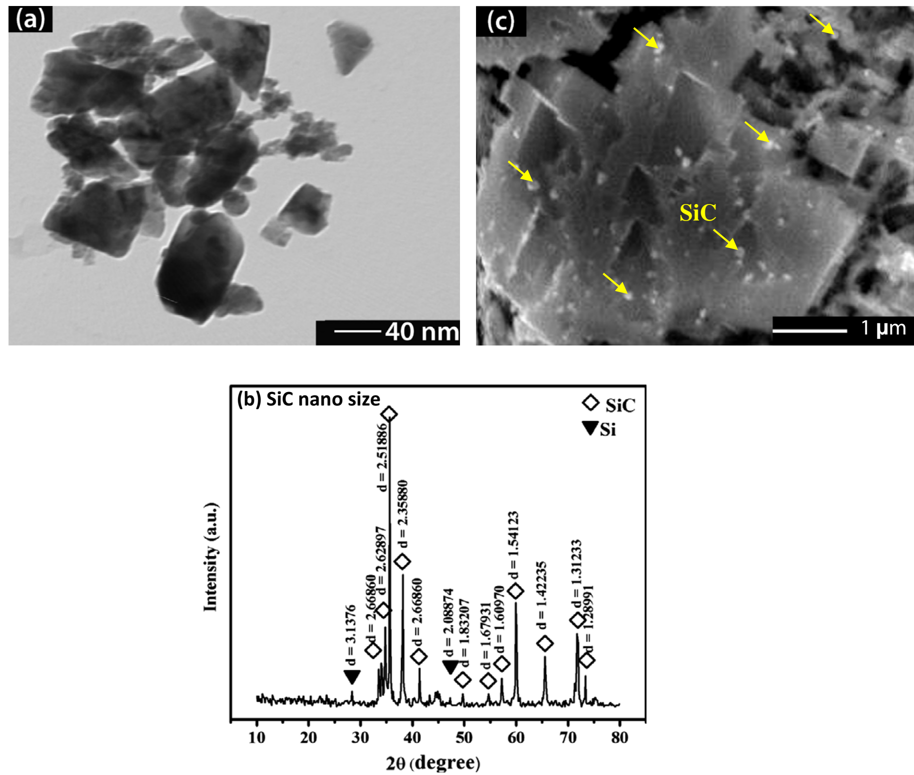

Fig. 1. (a) Bright field TEM of SiC nanoparticles and size distribution, (b) XRD patterns of nano-sized SiC particles and (c) spheroids and fine dot-shaped submicron SiC particles located on the surface of SAC(305)-0.7% SiC solder matrix.

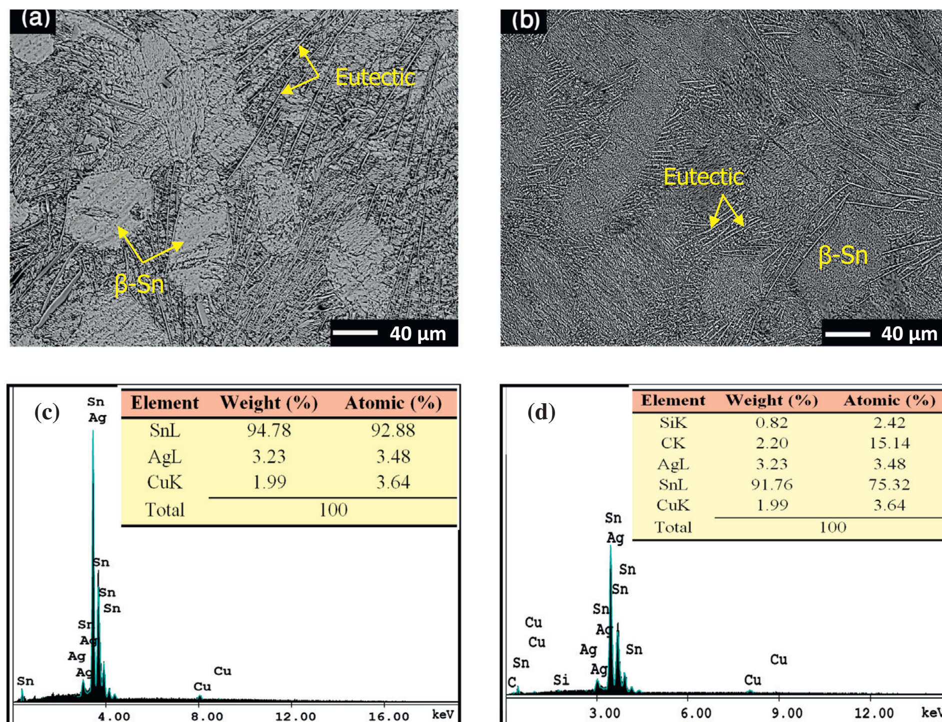

(c)

Element	Weight (%)	Atomic (%)
SnL	94.78	92.88
AgL	3.23	3.48
CuK	1.99	3.64
Total	100	

(d)

Element	Weight (%)	Atomic (%)
SiK	0.82	2.42
CK	2.20	15.14
AgL	3.23	3.48
SnL	91.76	75.32
CuK	1.99	3.64
Total	100	

Fig. 2. SEM micrographs of: (a) SAC305 solder, (b) SAC(305)-0.7%SiC solder, (c) EDS analysis of SAC305 solder and (d) EDS analysis of SAC(305)-0.7SiC solder.

particles with Cu_6Sn_5 and SiC nanoparticles. Recently, a similar tendency was reported for microstructure results of bulk SAC(105)-SiC composite solders [4–6]. This similar phenomenon was also found by Tsao [12], who reported that the notable effect of nano-TiO_2 particles on Pb-free Sn–3.5Ag–0.5Cu solder alloys is to refine the microstructure.

Please cite this article in press as: El-Daly AA et al. Microstructural modifications and properties of SiC nanoparticles-reinforced Sn–3.0Ag–0.5Cu solder alloy. J Mater Design (2014), http://dx.doi.org/10.1016/j.matdes.2014.08.058

ARTICLE IN PRESS

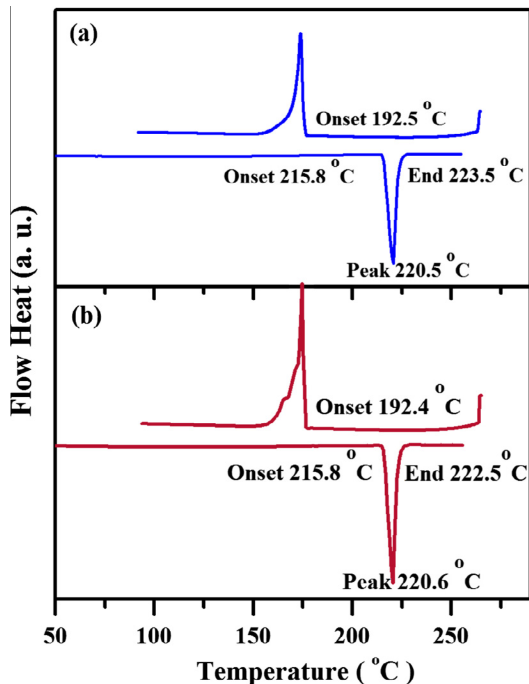

Fig. 3. DSC results during heating (endothermal) and cooling (exothermal) for (a) SAC305 and (b) SAC(305)-0.7%SiC solders.

3.3. Thermal behavior of SAC305 and SAC(305)-0.7% SiC solders

The process of solidification of solder alloys is a critical means for the final microstructure of solidified materials. Understanding the mechanism of solidification process of solder alloys, and how it is influenced by cooling process, temperature and alloying compositions, is crucial to the reliability of solder interconnections. DSC is a thermal analysis technique that can offer quantitative calorimetric results. Fig. 3 illustrates the DSC curves of SAC305 and SAC(305)-0.7% SiC through heating and cooling process. During heating, the solidus temperature T_{onset} appears at 215.8 °C with only one endothermic peak emerged at 220.5 and 220.6 °C for plain SAC305 and composite SAC(305)-0.7% SiC solders, respectively. These results show that addition of SiC has a little effect on the T_{onset} although the liquidus temperature (T_{end}) is slightly decreased by 1 °C with reinforcing SiC nanoparticles. The reason may be that the reinforcing nano-sized SiC particles could modify the surface instability and physical properties of grain boundary/interfacial characteristics. Such particles may serve as restrained sites for solidification process of IMCs as well as β-Sn grains [4–6]. The literature [13] shows that the addition of little amount of SiC particles (with an average size of 1 μm) did not appreciably affect the eutectic temperature of Sn–3.7Ag–0.9Zn solder. Moreover, these results are quite similar to those reported for SAC(355) and SAC(105) solders [6,11].

The pasty range, which is the difference between T_{end} and T_{onset} obtained in DSC analysis, is shown in Table 2. Remarkably, the pasty range occurs around 7.7 and 6.7 °C for SAC305 and SAC(305)-0.7% SiC solders, respectively. It appears that the pasty range is smaller than 11.5 °C for Sn–Pb solder alloys [14]. Such pasty range is likely to alleviate some manufacturing problems such as; the tendency toward porosity, hot tearing contraction during solidification and increasing the probability of fillet lifting phenomena.

Table 2
Solidus temperature (T_{onset}), liquidus temperature (T_{end}), pasty range and melting temperature for SAC(305) and SAC(305)-0.7SiC solder alloys from heating curve.

Alloy	(T_{onset}) (°C)	T_{end} (°C)	Pasty range (T_{end}–T_{onset}) (°C)	Melting temperature (°C)
SAC(305)	215.8	223.5	7.7	220.5
SAC(305)-0.7SiC	215.8	222.5	6.7	220.6

Undercooling is defined as the difference between the T_{onset} during heating and T_{onset} associated with cooling, and relates to the difficulty of nucleating the solid phase in a liquid state [6]. Several aspects could resolve the magnitude of undercooling. One of these factors is the structural characterization of solder. The other key factors imply the distribution of nanoparticles in the alloy matrix and their efficiency as nucleants. Yong-Jun and Bing-Bo [15] modeled the particle diameter dependent undercooling based on the classical theory of nucleation. They observed a significant change of undercooling and structural morphology of Cu–8Al alloy with the particle size. However, due to the undercooling, the exothermal peaks upon cooling for SAC305 and SAC(305)-0.7% SiC alloys appeared at lower temperatures when compared with their endothermal peaks, but the reductions in temperature were almost the same as seen in Fig. 3 and Table 3. Since the cooling speeds from melt can affect the degree of undercooling, therefore, the size and spacing, the morphology of the IMC particles as well as the β-Sn phase in SAC solder alloys would affect the degree of undercooling. For that reasons, the Ag_3Sn and Cu_6Sn_5 phases start to nucleate and start to grow. Nevertheless, the pseudo-eutectic of fine Ag_3Sn and Cu_6Sn_5 particles, followed by the β-Sn phase nucleate, thus hindering further growth of IMCs before reaching the equilibrium composition of eutectic phases.

Notably, the degree of undercooling for SAC305 solder was slightly increased from 23.3 to 23.4 °C although it is expected to decrease with SiC nanoparticles addition. In fact, a similar amount of undercooling may be supposed to affect the solidification processes of the other near-eutectic alloys, but probably not to the degree that it would change the observed primary phases. Hence, these solidification-microstructure observations provide a preliminary correlation with some features of their phase diagram. However, the mechanism of highest undercooling corresponds to the smallest particle size shown in Fig. 2b. These results propose that the undercooling achieved in DSC analysis is strongly dependent on the undissolved SiC nanoparticles in SAC 305 solder. The observed phenomenon of increasing the degree of undercooling with decreasing particle size of IMCs may be attributed to several issues. For instance, a pseudo homogeneous nucleation mechanism may be operating and expected at the small length scales in Sn crystals, and therefore would be the probability of crystal nucleation.

3.4. General tensile tests

Fig. 4 shows the mechanical properties of SAC305 and SAC(305)-0.7% SiC solders at strain rate of 1×10^{-2} s^{-1}. The entire data are plotted at temperatures 25 °C and 75 °C and the tensile parameters such as; elastic modulus *E*, yield stress 0.2%YS, ultimate tensile strength UTS, and total elongation El are compiled below in the corresponding histograms. As seen, the two solders show similar trend with deformation temperature effect although SiC addition tends to increase both the UTS and 0.2% YS of SAC(103) solder, while lowering the percent of elongation. When the tensile tests are performed at 75 °C for both alloys, the solder creep effect is significant. So, the results of this elevated-temperature test indicated a drop of at most half of the values of *E*, 0.2%YS and UTS at low-temperature measurements, while the percent of elongation increases nearly two times. However, these results are incredibly similar to the previous findings [4,16] that the tensile behavior of SAC alloys often exhibits a strong dependence on temperature. Several plausible reasons

Please cite this article in press as: El-Daly AA et al. Microstructural modifications and properties of SiC nanoparticles-reinforced Sn–3.0Ag–0.5Cu solder alloy. J Mater Design (2014), http://dx.doi.org/10.1016/j.matdes.2014.08.058

ARTICLE IN PRESS

Table 3
Undercooling range for SAC(305) and SAC(305)-0.7SiC solder alloys.

Alloy	(T_{onset}) heating (°C)	T_{onset} cooling (°C)	Undercooling (°C)
SAC(305)	215.8	192.5	23.3
SAC(305)-0.7SiC	215.8	192.4	23.4

subsist for mechanical strength sensitivity to the testing temperatures. These include the nature of interface formed between the nanoparticles and matrix, compositional and heat treatment effects on the matrix phase, the stability of soft and hard IMCs in the alloy matrix and the change of processing parameters. A comparison of tensile parameters of SAC305 and SAC(305)-0.7% SiC solders at room temperature with some SAC lead-free solders [4,17–20] reveals a comparable behavior as seen in Table 4.

3.5. Fracture surface analysis

Fig. 5 shows the typical fracture surfaces of tensile specimens of SAC305 and nano-composite SAC(305)-0.7% SiC samples tested at room temperature and strain rate of 10^{-2} s^{-1}. Notably, typical ductile fracture mode with the characteristic of dimples has been observed for specimens with and without SiC nanoparticles addition. Since the dimples are a result of micro-voids coalescence, the typical cup and cones fracture mode are normally happened in ductile materials, these dimples are usually equiaxed in shape as shown in Fig. 5a and b. Generally, the larger and deeper dimple is, the better plastic property is [5]. Fig. 5a shows that the fracture

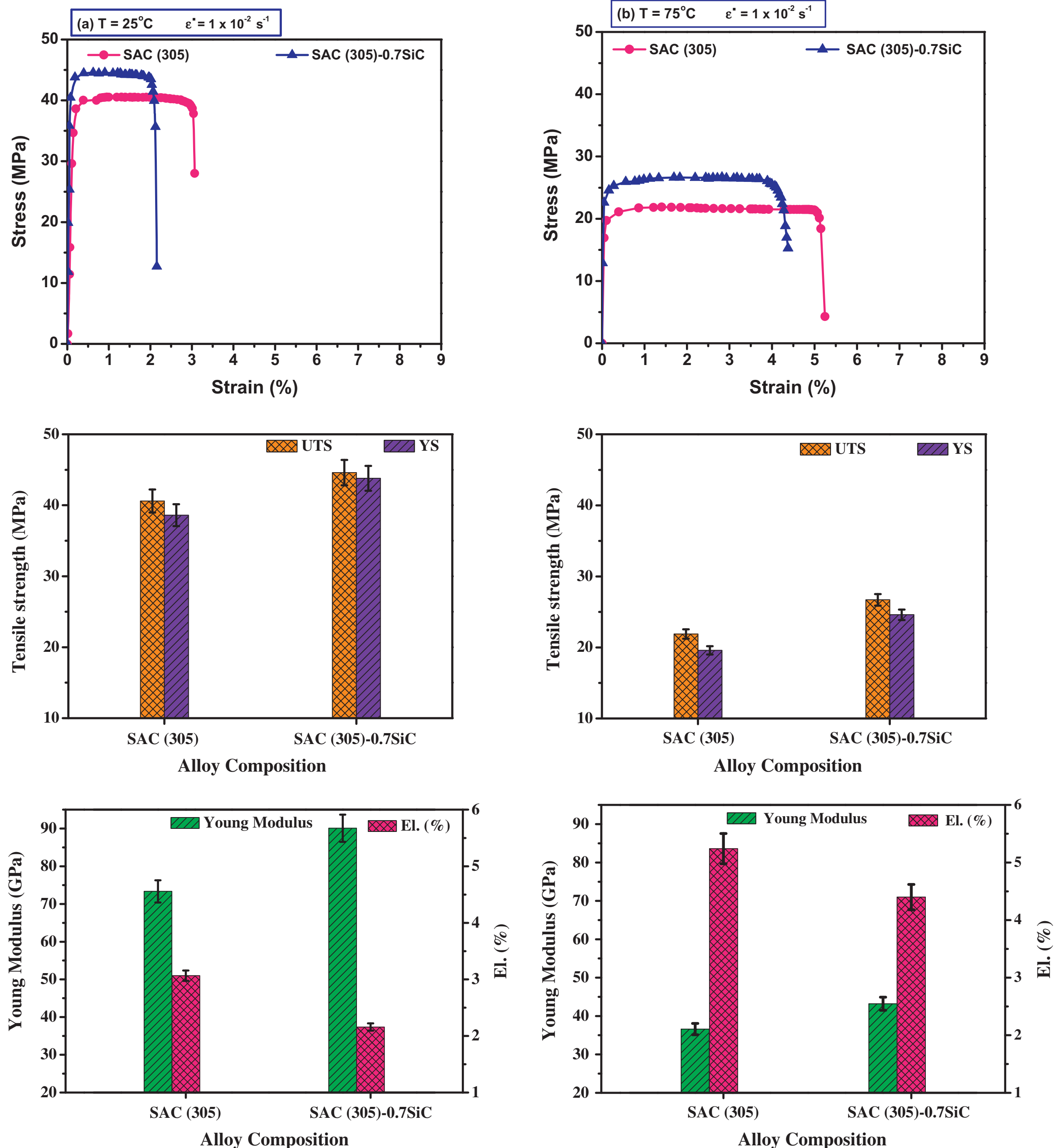

Fig. 4. Tensile properties of SAC305 and SAC(305)-0.7%SiC solder alloys at strain rate of 1×10^{-2} s^{-1} and temperature: (a) T = 25 °C and (b) T = 75 °C.

Please cite this article in press as: El-Daly AA et al. Microstructural modifications and properties of SiC nanoparticles-reinforced Sn–3.0Ag–0.5Cu solder alloy. J Mater Design (2014), http://dx.doi.org/10.1016/j.matdes.2014.08.058

ARTICLE IN PRESS

Table 4
Comparison of tensile properties of SAC (305) and SAC(305)-0.7SiC solder alloys with some references at room temperature.

Alloy	Elastic modulus (GPa)	UTS (MPa)	0.2%YS (MPa)	Elongation (%)
SAC(305)	73.33	40.6	38.6	3.1
SAC(305)-0.7SiC	90.07	44.6	43.8	2.2
SAC(105) [4]	–	30.0	28.8	12.3
SAC(105)-0.35SiC [4]	–	33.2	31.3	13.0
SAC(305) [18]	60.0	47.0	28.8	12.3
SAC(405) [19]	–	45.0	38.0	–
SAC(305)-0.6TiO_2 [20]	–	48.9	38.0	–

mode clearly appeared to have a coarse surface, shiny IMCs and large dimples on the surface of fracture solder. Accordingly, the fracture surfaces of SAC305 appeared to be ductile. But, the addition of SiC nanoparticles dramatically changed the fracture mode of SAC305 solder. Fig. 5b shows that the fracture mode clearly appeared to have a relatively fine surface, shiny IMCs with small dimples on the surface of fracture solder. The fracture surface of composite solder appeared to be less ductile with very fine dimple surface than the plain solder. As expected during solidification, the SiC nanoparticles acted as nucleation sites of primary β-Sn matrix and resulted in fine microstructure due to the homogeneous distribution of SiC particles.

3.6. Effect of strain rate on the mechanical properties of solders

Fig. 6 shows the effect of strain rate on tensile parameters of SAC305 and SAC(305)-0.7% SiC solder specimens at $T = 25\,°C$. Results show that both the strain rate and SiC-addition remarkably affect the tensile parameters. The values of E, 0.2% YS and UTS of

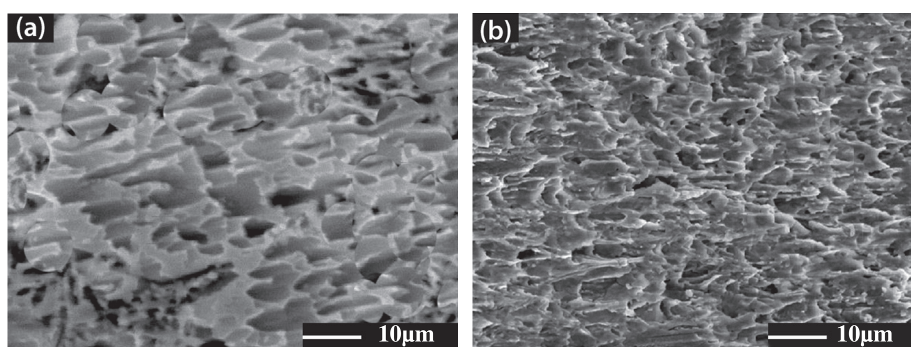

Fig. 5. Typical fracture surfaces of (a) SAC305 and (b) SAC(305)-0.7SiC solders.

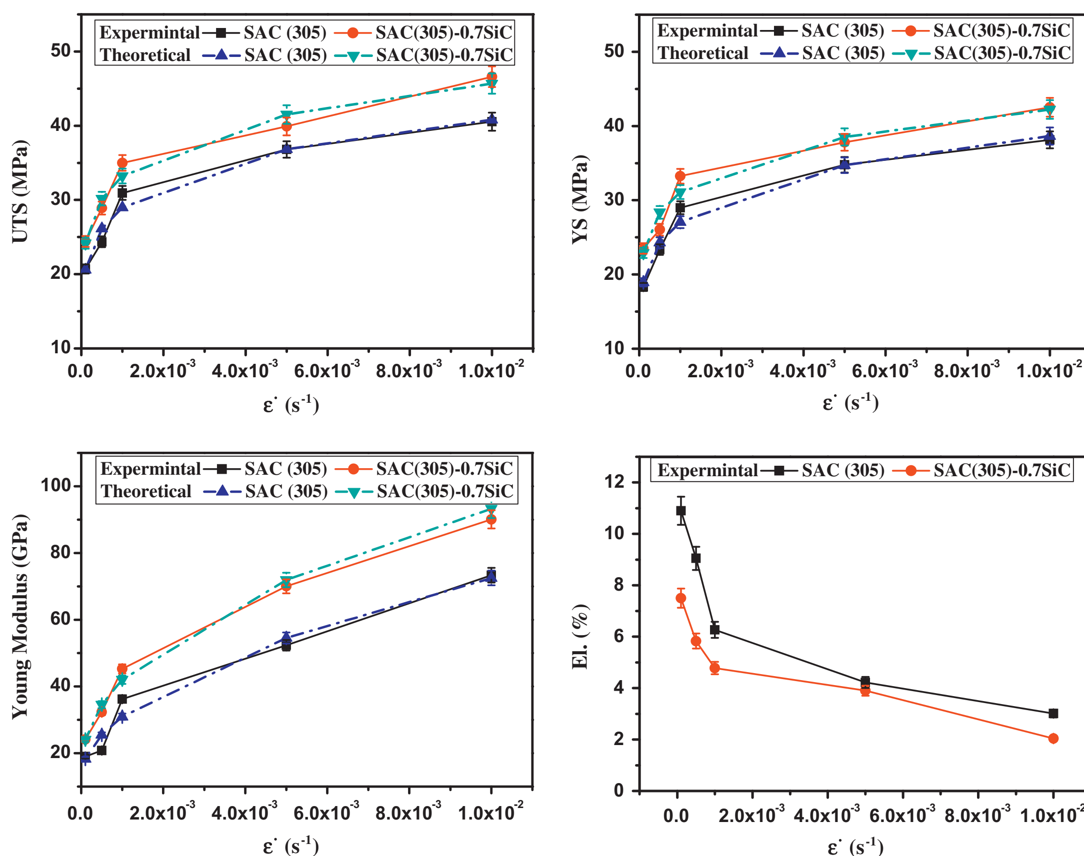

Fig. 6. Experimental and theoretical mechanical property data for SAC305 and SAC(305)-0.7%SiC solder alloys at room temperature and various strain rates.

Please cite this article in press as: El-Daly AA et al. Microstructural modifications and properties of SiC nanoparticles-reinforced Sn–3.0Ag–0.5Cu solder alloy. J Mater Design (2014), http://dx.doi.org/10.1016/j.matdes.2014.08.058

ARTICLE IN PRESS

Table 5
Material constants in the rate-dependent mechanical properties models of (1)–(3).

Solders	a_1 (GPa)	a_2	a_3 (GPa)	b_1 (MPa)	b_2	c_1 (MPa)	c_2
SAC(305)	647.3	0.5176	12.83	78.93	0.155	80.97	0.1487
SAC(305)-0.7SiC	643.8	0.4562	14.49	77.80	0.1327	86.44	0.1384

both solders are gradually increased as the deformation rate increased although the elongation is decreased. With the addition of 0.7% SiC to SAC305 solder, the E, 0.2% YS and UTS values are increased. Notably, the elastic modulus of SAC(305)-0.7% SiC solder is 12.75% higher than that of plain SAC305 solder at all strain rate investigated, whereas the 0.2% YS and UTS values are enhanced by 11.4%. Such change in elastic modulus and mechanical strength can be designated by microstructural changes observed in Fig. 2. The SAC(305)-0.7% SiC alloy displayed a fine eutectic IMC particles dispersed in β-Sn matrix as a result of SiC addition. The enhanced mechanical response by SiC addition was also reported by El-Daly et al. [4–6], who pointed out that the IMC size did not constantly decrease with increasing amount of SiC nanoparticles in the SAC(105)solder and the composite solder containing 0.35 wt.% SiC nanoparticles only have identical behavior. Consistent with the Orowan theory, the mechanical strength of solder matrix is inversely proportional to the interparticle spacing, which agrees with the dispersion strengthening mechanism. However, the enhancement of tensile parameters with increasing strain rate is in good agreement with the result reported for SAC and SC solders by Chen et al. [20] and El-Daly et al. [4]. The decrease in elongation with increasing strain rate may be attributed to the unrecoverable plastic deformation capacity caused by high strain rates. These results also propose that high strain rate sensitivities are necessary to create high strain rate plasticity.

Based on the experimental results, the strain rate-dependent material property models of SAC305 based-solders including E, 0.2%YS and UTS can be written as the following empirical relations:

$$E(\dot{\varepsilon}) = a_1(\dot{\varepsilon})^{a_2} + a_3 \quad (1)$$

$$\mathrm{YS}(\dot{\varepsilon}) = b_1(\dot{\varepsilon})^{b_2} \quad (2)$$

$$UTS(\dot{\varepsilon}) = c_1(\dot{\varepsilon})^{c_2} \quad (3)$$

where a_1, a_2, a_3, b_1, b_2, c_1 and c_2 are material constants, which are obtained from the nonlinear regression and listed in Table 5. The calculated values of tensile parameters compared with experimental results are shown in Fig. 6 and listed in Table 6. A good agreement between the experimental data and the model predictions is achieved for strain rate ranges at 25 °C. It is seen that the theoretical models are accurate with an errors within 1.1–3.2% for the predicted elastic modulus, 0.02–0.04% for the predicted yield stress and 0.07% for the predicted UTS.

3.7. Effect of temperature on the mechanical properties

Fig. 7 shows the effect of testing temperature on tensile properties of both solders at strain rate of 1.0×10^{-3} s^{-1}. It is clear that both solders become more ductile and softer when testing temperature increases. The UTS and 0.2% YS decrease with increasing temperature although the ductility, as measured by percent elongation, has increased. The effect of temperature on the mechanical properties of two solders at high temperatures is more prominent compared with such effect at low temperatures. This means that the dynamic recovery process is more significant at higher temperatures and fixed strain rate. The main observation through these tensile tests is that the highest UTS and 0.2% YS arise with the SAC(305)-0.7% SiC composite samples at all temperature range investigated. The composite SAC(305)-0.7% SiC solder has an 0.2% YS and UTS about 20% and 15% higher than that of SAC305 alloy. Generally, the strengthening mechanism of composite SAC(305)-0.7% SiC solder may be contributed to many reasons including; the Hall–Petch effect due to sub-grain size refinement, Orowan strengthening mechanism due to the presence of SiC nanoparticles with small spacing inside solder matrix, the generation of geometrically necessary dislocations to accommodate CTE mismatch between the matrix and small particles and load bearing effects due to the presence of nano-sized reinforcements [4].

Table 6
Experimental and theoretical mechanical property data for different solders at various strain rates.

Solders/strain rate (s^{-1})	Experimental values			Theoretical values		
	E (GPa)	Yield (MPa)	UTS (MPa)	E (GPa)	Yield (MPa)	UTS (MPa)
SAC (305)						
1.0E−5	–	–	–	14.50	13.25	14.62
5.0E−5	–	–	–	16.67	17.01	18.57
1.0E−4	19.02	18.31	20.7	18.33	18.93	20.58
5.0E−4	20.85	23.35	24.36	25.49	24.29	26.15
1.0E−3	36.24	28.99	30.94	30.95	27.05	28.99
5.0E−3	52.38	34.78	36.81	54.52	34.72	36.82
1.0E−2	73.33	38.13	40.55	72.52	38.66	40.82
5.0E−2	–	–	–	150.13	49.61	51.86
1.0E−1	–	–	–	209.39	55.24	57.49
SAC(305)-0.7SiC						
1.0E−5	–	–	–	17.86	16.88	17.56
5.0E−5	–	–	–	21.51	20.90	21.95
1.0E−4	24.18	23.51	24.41	24.13	22.91	24.16
5.0E−4	32.38	26.04	28.90	34.57	28.37	30.18
1.0E−3	45.28	33.24	34.99	42.04	31.10	33.22
5.0E−3	70.01	37.81	39.90	71.90	38.51	41.51
1.0E−2	94.07	42.52	46.60	93.25	42.22	45.69
5.0E−2	–	–	–	178.63	52.27	57.10
1.0E−1	–	–	–	239.68	57.31	62.85

Please cite this article in press as: El-Daly AA et al. Microstructural modifications and properties of SiC nanoparticles-reinforced Sn–3.0Ag–0.5Cu solder alloy. J Mater Design (2014), http://dx.doi.org/10.1016/j.matdes.2014.08.058

ARTICLE IN PRESS

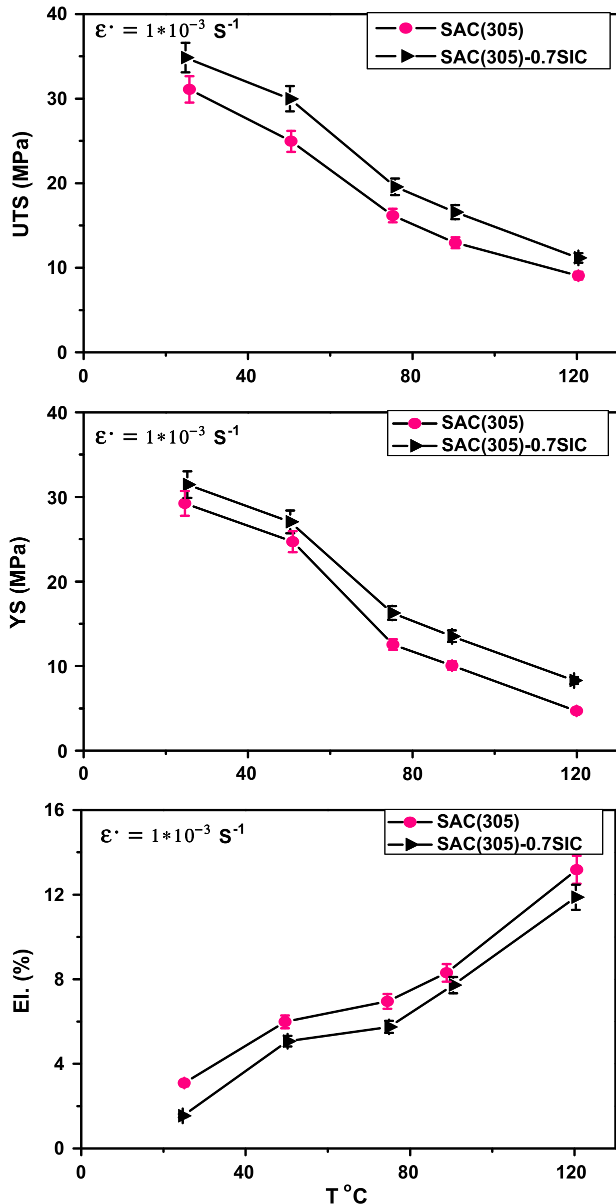

Fig. 7. Effect of temperature on ultimate tensile strength (UTS), yield stress (0.2%YS) and elongation (El.%) at strain rate of $1 \times 10^{-3}\,s^{-1}$ for SAC305 and SAC(305)-0.7%SiC solder alloys.

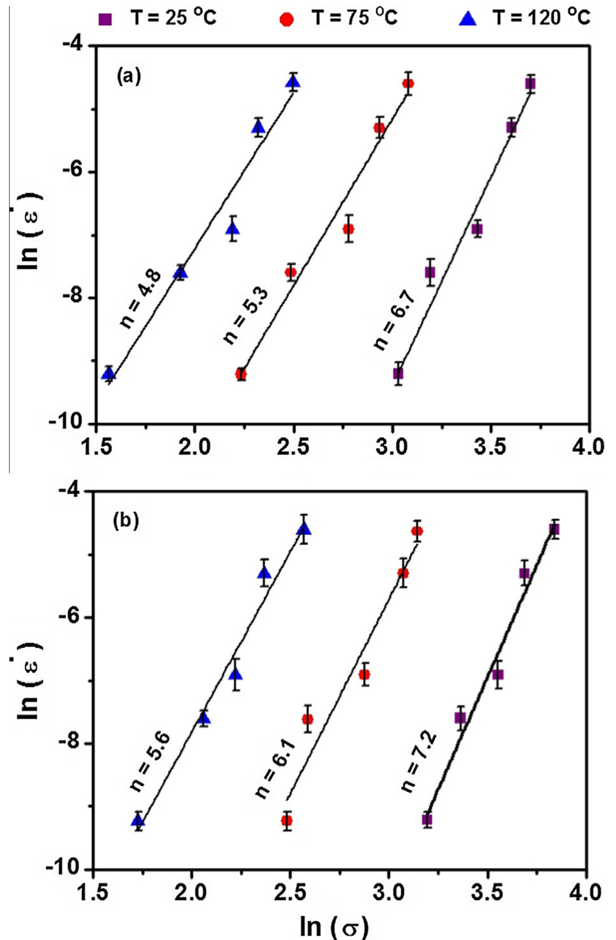

Fig. 8. Relationship between ln (σ) and ln $(\varepsilon^{\bullet})$ for calculation of n values at different temperatures for (a) SAC305 and (b) SAC(305)-0.7%SiC solder alloys.

3.8. Kinetic analysis of SAC305-based solders during hot deformation

According to the well known Dorn power law equation [21]:

$$\acute{\varepsilon} = A\sigma^n \exp(-Q/RT) \quad (4)$$

where A is a constant; R is the universal gas constant; n is the stress exponent constant related to strain rate $\acute{\varepsilon}$; T (K) is thermodynamic deformation temperature; σ (MPa) means peak stress or UTS; Q (kJ/mol) is the activation energy of deformation. The change in stress exponent (n) and activation energy (Q) values associated with the deformation of crystalline materials at temperatures above $0.5T_m$ (where T_m is the melting temperature), can be used to identify the mechanisms controlling the deformation process. Approximate values of n were calculated according to Eq. (4) from the slope of each line shown in Fig. 8. Similarly, the activation energy Q of entire solders are calculated by linear regression of experimental data relating $\ln(\sigma)$ and $1/T$ (Fig. 9). The parameters are summarized in Table 7. It can be seen that the composite SAC(305)-0.7% SiC solder alloy has higher stress exponent values than the plain SAC305 solder, since the microstructure is finer in case of the former than in the latter. According to the classical heterogeneous nucleation theory, SiC nanoparticles will diminish the thermodynamic barrier of β-Sn nucleation in order to enhance the nucleation rate of IMC particles and refine β-Sn grain size. Consequently, it can strengthen the mechanical properties of composite solder. However, the n-values are decreased from 6.7 and 7.2 at 25 °C to 4.8 and 5.6 at 120 °C for both solders, respectively. The reduction of n-value has been related to the instability of the microstructure, which occurs at high deformation temperatures [16,17]. These results are well agreed with that reported for some composite SAC solders [4,6].

Although several mechanisms [22] such as dislocation mechanism, grain boundary sliding and diffusion mechanism have been proposed for deformation of crystalline materials such as Pb free solder alloys, dislocation mechanism seems to be the most appropriate in the present study as confirmed by the stress exponents values between 4.8 and 7.2 in both alloys. In this mechanism, the tensile deformation behavior is controlled by dislocation climb related processes. As well, the improvement in mechanical strength with the addition of SiC nanoparticles can be ascribed to the interactions of dislocations with these nanoparticles, which obstructed the dislocation climb. These interactions are also confirmed by the increase in Q value from 76.6 kJ mol^{-1} to 84.7 kJ mol^{-1} with the addition of SiC nanoparticles, as seen in Table 7. The activation energies of 76.6 and 84.7 kJ mol^{-1} are more close to that of lattice self-diffusion of β-Sn (67–73 kJ mol^{-1}), and

Please cite this article in press as: El-Daly AA et al. Microstructural modifications and properties of SiC nanoparticles-reinforced Sn–3.0Ag–0.5Cu solder alloy. J Mater Design (2014), http://dx.doi.org/10.1016/j.matdes.2014.08.058

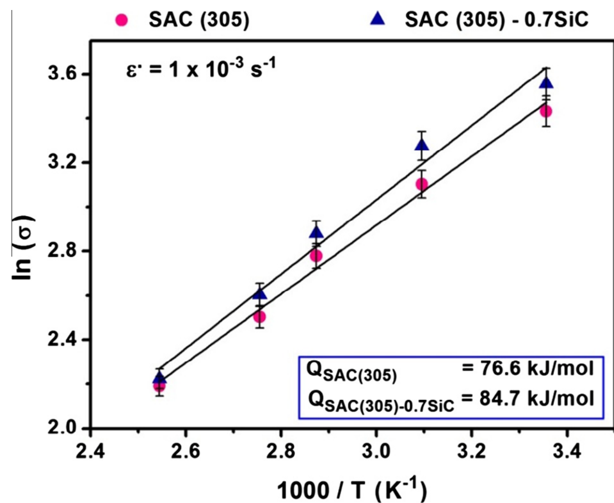

Fig. 9. The activation energy (Q) values of SAC305 and SAC(305)-0.7%SiC solder alloys.

Table 7
Activation energy (Q) and stress exponent (n) values for SAC(305) and SAC(305)-0.7SiC solder alloys.

Alloy	Q (kJ/mol)	Temperature (°C)	n
SAC(305)	76.6	25	6.7
		70	5.3
		120	4.8
SAC(305)-0.7SiC	84.7	25	7.2
		70	6.1
		120	5.6

thus, it can be proposed that the dominant deformation mechanism in these alloys is dislocation climb [22].

4. Conclusions

This study investigates the effect of an addition of 0.7 wt.% SiC nanoparticles on microstructure, melting property and mechanical properties of Sn–3.0Ag–0.5Cu lead-free solder alloy. Experimental results revealed that the nano-sized SiC particles has significantly refined the microstructure of composite SAC(305)-0.7% SiC solder, increased the strength and elastic modulus in comparison with the plain SAC305 alloy casting. In addition, SiC particles decrease their pasty range although the undercooling and eutectic temperature prolonged nearly at the SAC305 level. A strain rate-dependent model of elastic modulus (E), yield stress (0.2%YS) and ultimate tensile strength (UTS) was developed based on the test results. The predicted tensile parameters for both solders are reasonably close to the present experimental data. According to the obtained n and Q values, it is suggested that the dominant deformation mechanism in both solder alloys is the dislocation climb over the whole temperature range investigated. Remarkably, the difference in n and Q values for both alloys is due to the difference in the as-solidified microstructures owing to SiC nanoparticles addition.

References

[1] Gain AK, Chan YC. Growth mechanism of intermetallic compounds and damping properties of Sn–Ag–Cu-1 wt% nano-ZrO_2 composite solders. Microelectron Reliab 2014;54:945–55.

[2] Lazarova R, Petrov RH, Gaydarova V, Davidkov A, Alexeev A, Manchev M, et al. Microstructure and mechanical properties of P265GH cast steel after modification with TiCN particles. Mater Des 2011;32:2734–41.

[3] Liu P, Yao P, Liu J. Effect of SiC nanoparticle additions on microstructure and microhardness of Sn–Ag–Cu solder alloy. J Electron Mater 2008;37(6):874–9.

[4] El-Daly AA, Fawzy A, Mansour SF, Younis MJ. Thermal analysis and mechanical properties of Sn–1.0Ag–0.5Cu solder alloy after modification with SiC nano-sized particles. J Mater Sci: Mater Electron 2013;24:2976–88.

[5] El-Daly AA, Fawzy A, Mansour SF, Younis MJ. Novel SiC nanoparticles-containing Sn–1.0Ag–0.5Cu solder with good drop impact performance. Mater Sci Eng, A 2013;578:62–71.

[6] El-Daly AA, Al-Ganainy GS, Fawzy A, Younis MJ. Structural characterization and creep resistance of nano-silicon carbide reinforced Sn–1.0Ag–0.5Cu lead-free solder alloy. Mater Des 2014;55:837–45.

[7] Shen J, Liu YC, Wang DJ, Gao HX. Nano ZrO_2 particulate-reinforced lead-free solder composite. J Mater Sci Technol 2006;22:529–32.

[8] Tsao LC, Chang SY. Effects of nano-TiO_2 additions on thermal analysis, microstructure and tensile properties of Sn3.5Ag0.25Cu solder. Mater Des 2010;31:990–3.

[9] Tsao LC, Chang SY, Lee CI, Sun WH, Huang CH. Effects of nano-Al_2O_3 additions on microstructure development and hardness of Sn3.5Ag0.5Cu solder. Mater Des 2010;31:4831–5.

[10] Chuang TH, Wu MW, Chang SY, Ping SF, Tsao LC. Strengthening mechanism of nano-Al_2O_3 particles reinforced Sn3.5Ag0.5Cu lead-free solder. J Mater Sci: Mater Electron 2011;22:1021–7.

[11] Fawzy A, Fayek SA, Sobhy M, Nassr E, Mousa MM, Saad G. Effect of ZnO nanoparticles addition on thermal, microstructure and tensile properties of Sn–3.5 Ag–0.5 Cu (SAC355) solder alloy. J Mater Sci: Mater Electron 2013;24:3210–8.

[12] Tsao LC. An investigation of microstructure and mechanical properties of novel Sn3.5Ag0.5Cu–XTiO_2 composite solders as functions of alloy composition and cooling rate. Mater Sci Eng, A 2011;529:41–8.

[13] Wang X, Liu YC, Wei C, Gao HX, Jiang P, Yu LM. Strengthening mechanism of SiC-particulate reinforced Sn–3.7Ag–0.9Zn lead-free solder. J Alloys Compds 2009;480:662–5.

[14] El-Daly AA, Hammad AE, Al-Ganainy GS, Ragab M. Properties enhancement of low Ag-content Sn–Ag–Cu lead-free solders containing small amount of Zn. J Alloys Compds 2014;614:20–8.

[15] Yong-Jun L, Bing-Bo W. A transient from eutectic growth to dendritic growth induced by high undercooling conditions. Chin Phys Lett 2003;20(8):1379–85.

[16] El-Daly AA, El-Taher AM, Dalloul TR. Enhanced ductility and mechanical strength of Ni-doped Sn–3.0Ag–0.5Cu lead-free solders. Mater Des 2014;55:309–18.

[17] Che FX, Zhu WH, Poh EXW, Zhang XW, Zhang XR. The study of mechanical properties of Sn–Ag–Cu lead-free solders with different Ag contents and Ni doping under different strain rates and temperatures. J Alloys Compds 2010;507:215–24.

[18] Su YA, Tan LB, Tee TY, Tan VBC. Rate-dependent properties of Sn–Ag–Cu based lead-free solder joints for WLCSP. Microelectron Reliab 2010;50:564–76.

[19] Tang Y, Li GY, Pan YC. Effects of TiO_2 nanoparticles addition on microstructure, microhardness and tensile properties of Sn–3.0Ag–0.5Cu–xTiO_2 composite solder. Mater Des 2014;55:574–82.

[20] Chen WM, Kang SK, Kao CR. Effects of Ti addition to Sn–Ag and Sn–Cu solders. J Alloys Compds 2012;520:244–9.

[21] El-Daly AA, Hammad AE, Al-Ganainy GS, Ibrahiem AA. Design of lead-free candidate alloys for low-temperature soldering applications based on the hypoeutectic Sn–6.5Zn alloy. Mater Des 2014;56. 594–03.

[22] Mahmudi R, Geranmayeh AR, Zahiri M, Marvasti H. Effect of rare earth element additions on the impression creep of Sn–9Zn solder alloy. J Mater Sci: Mater Electron 2010;21:58–64.

Please cite this article in press as: El-Daly AA et al. Microstructural modifications and properties of SiC nanoparticles-reinforced Sn–3.0Ag–0.5Cu solder alloy. J Mater Design (2014), http://dx.doi.org/10.1016/j.matdes.2014.08.058